Microbiology Spectrum

| Open Peer Review | Computational Biology | Research Article

Modeling dynamic oxygen permeability as a mechanism to mitigate oxygen-induced stresses on photosynthesis and N_2 fixation in marine *Trichodesmium*

Weicheng Luo,[1,2,3] Keisuke Inomura,[4] Ondřej Prášil,[2] Meri Eichner,[2] Ya-Wei Luo[1]

AUTHOR AFFILIATIONS See affiliation list on p. 15.

ABSTRACT *Trichodesmium*, the predominant marine diazotrophic cyanobacterium, concurrently performs nitrogen (N_2) fixation and photosynthesis, the latter of which produces oxygen (O_2) that inhibits N_2 fixation. Hopanoid lipids in *Trichodesmium* may play a role in dynamically regulating membrane permeability to O_2, potentially alleviating O_2 stress on N_2 fixation. However, the physiological impacts of this dynamic permeability are not well understood. We developed a model showing that dynamically modulating membrane O_2 permeability can enhance N_2 fixation and growth of *Trichodesmium* by over 50%. High O_2 permeability (1.5×10^{-4} of O_2 diffusivity in seawater) during strong photosynthesis accelerates O_2 exhaust, reducing energy-consuming photorespiration by ~40%, while low O_2 permeability (1.0×10^{-5} diffusivity) during active N_2 fixation minimizes O_2 stress on N_2 fixation. Together, these mechanisms increase the carbon and iron use efficiencies by ~70%. Our study provides a mechanistic and quantitative framework for how dynamic O_2 permeability benefits *Trichodesmium*, offering insights potentially applicable to other diazotrophs.

IMPORTANCE *Trichodesmium* is a key player in marine N_2 fixation, essential for oceanic productivity and global biogeochemical cycles. However, a significant challenge arises from the concurrent photosynthetic production of O_2 during N_2 fixation, which can inhibit N_2 fixation and cause energy-wasting photorespiration. We develop a physiological model showing that *Trichodesmium* may dynamically regulate membrane O_2 permeability to enhance N_2 fixation and growth. The model suggests two mechanisms: elevated O_2 permeability during the early daytime of strong photosynthesis accelerates O_2 exhaust to the environment, reducing photorespiration, while reduced O_2 permeability later limits O_2 influx from the environment, lowering wasteful respiration and maintaining a low intracellular O_2 level for active N_2 fixation. These adaptations improve the efficiency of carbon and iron utilization, thereby facilitating N_2 fixation and growth in *Trichodesmium*. This study sheds light on how *Trichodesmium* and other N_2-fixing microorganisms can optimize their physiological processes in response to environmental challenges.

KEYWORDS *Trichodesmium*, dynamic oxygen permeability, nitrogen fixation, photorespiration, respiratory protection

Trichodesmium is a major photoautotrophic contributor to marine nitrogen (N_2) fixation (1–3). *Trichodesmium* faces physiological challenges, such as the decrease in the activity of nitrogenase (the enzyme for N_2 fixation) upon exposure to oxygen (O_2) (4–6). Given that *Trichodesmium* simultaneously conducts N_2 fixation and O_2-producing photosynthesis during the daytime (4, 7), *Trichodesmium* has developed several physiological strategies to cope with this O_2 stress on nitrogenase and protect N_2

Editor Hongan Long, Ocean University of China, Qingdao, Shandong, China

Peer Reviewer Nir Keren, Hebrew University of Jerusalem, Jerusalem, Israel

Address correspondence to Weicheng Luo, weicheng123@stu.xmu.edu.cn, or Ya-Wei Luo, ywluo@xmu.edu.cn.

The authors declare no conflict of interest.

Received 24 February 2025
Accepted 23 June 2025
Published 13 August 2025

fixation (8). One of these is the respiratory protection: *Trichodesmium* creates a low-O_2 intracellular environment to realize sufficient N_2 fixation by temporally segregating photosynthesis and N_2 fixation and wastefully respiring organic carbon with intracellular O_2 (9–11). A potentially complementary strategy is the diffusion adjustment; a proper low cell membrane permeability to O_2 can contribute to forming and maintaining the low-O_2 window (10, 12, 13).

Notably, during the early light period with high rates of photosynthesis and O_2 production, low cell permeability to O_2 could lead to high intracellular O_2 concentrations, resulting in oxidative stress on photosynthesis as well as photorespiration, an energy-inefficient consumption of O_2 (10, 13, 14). Photorespiration is a light-dependent process that consumes ATP (adenosine triphosphate), NADPH (nicotinamide adenine dinucleotide phosphate hydrogen), reduced N and O_2, and produces CO_2 (15). This oxygenation reaction is catalyzed by RuBisCO (ribulose-1,5-bisphosphate carboxylase/oxygenase) with RuBP (ribulose-1,5-bisphosphate) and O_2 as substrates (15). Consequently, the high intracellular O_2 concentration during early daytime can compete with CO_2 and inhibit the carboxylation activity of RuBisCO, thus increasing photorespiration and reducing photosynthetic carbon fixation (13, 14, 16). While cyanobacteria are known to operate carbon concentrating mechanisms (CCM) to increase intracellular CO_2 concentration and thus shift the CO_2:O_2 ratio in favor of carboxylation rather than oxygenation, recent studies have suggested that photorespiration may still play an important role in these organisms (17). Technical difficulties have so far hindered direct quantification of photorespiration rates in cyanobacteria, and given these uncertainties, photorespiration has not been explicitly resolved in previous models of *Trichodesmium* (10, 12, 13).

Due to the importance of O_2 concentration on the likelihood of photorespiration, the permeability of the cell membrane to O_2 may impact the occurrence of photorespiration. For example, a high cell permeability to O_2 could facilitate the rapid diffusion of intracellular O_2 to the extracellular environment, likely decreasing the photorespiration rate during the early light period when photosynthesis is strong in *Trichodesmium* (14). This high O_2 permeability could also enhance the diffusion rate of extracellular O_2 into the cytoplasm during the low-O_2 window, thereby elevating the respiratory protection required to consume organic carbon and intracellular O_2 as an indirect cost for N_2 fixation (10). On the contrary, a low cell permeability to O_2 would elevate the photorespiration but benefit N_2 fixation. The above scenarios are based on the assumption of diurnally constant cell permeability to O_2, as employed in previous model studies (10, 12, 13). However, *Trichodesmium* can synthesize hopanoids, which can be intercalated into lipid bilayers of membranes (18, 19). The planar and hydrophobic structure of hopanoids may decrease the membrane permeability to O_2. Also, hopanoids may form rafts (high concentration domain), which can be distributed within the membrane, and thus may dynamically regulate cell permeability to O_2 (dynamic-permeability model case) (18, 20). Such a dynamic regulation is currently a hypothesis; it is likely that the dynamic expression of hopanoid biosynthesis genes may occur, given the highly dynamic protein expression in *Trichodesmium* (21). The potential physiological implications of this dynamic cell permeability to O_2 (DPO_2) to *Trichodesmium* remain poorly understood and warrant further investigation.

In this study, we hypothesize that DPO_2 helps to regulate intracellular O_2 levels and mitigates O_2-induced stresses in *Trichodesmium*, promoting the efficiency of key enzymes such as RuBisCO and nitrogenase in the context of temporally segregating the activities of the two enzymes. To test the hypothesis, we improved previous models by representing more processes, including photorespiration and DPO_2. The analyses of the model results, along with the comparison to additional experiments of fixed O_2 permeability, which was set diurnally constant (fixed-permeability model case), provided a mechanistic and quantitative understanding of the potential role of DPO_2 in impacting photorespiration and N_2 fixation in *Trichodesmium*.

MATERIALS AND METHODS

The model in this study was developed by incorporating new representations of photorespiration and DPO_2 into previous models (10, 22). In the subsequent sections, we present a concise overview of the model structure. We provide more detailed descriptions, parameter values, intermediate variables, and state variables in Supplementary Methods and Table S1 to S3.

General model framework

The model (Fig. 1A) simulates key physiological processes in *Trichodesmium* trichome, including photosynthetic electron transfer (PET), carbon fixation, photorespiration, and N_2 fixation over a 12 hour diurnal cycle. These processes are modulated by the dynamic allocation of Fe, ATP, and NADPH to different metabolic pathways, as well as by intracellular O_2 management (Fig. 1A). Two pathways of PET are represented, including linear PET (LPET) that produces ATP and NADPH, and alternative electron transfer (AET) that only generates ATP. ATP and NADPH are used in various processes as described below. N_2 fixation occurs only when intracellular O_2 is low. Photorespiration increases with increasing intracellular O_2 levels.

Photosynthetic pathways

The photosynthetic pathways followed previous model schemes (10, 22). The total rate of PET is positively regulated by light intensity and the Fe allocated to photosystems. Conversely, it is mitigated by respiratory protection mechanisms (4). The proportion of electrons directed toward linear PET (LPET) and alternative electron transport (AET) is computed at each time step. This is assumed to meet the immediate intracellular requirements for ATP and/or NADPH (10, 22).

O_2 production and dynamic permeability

O_2 is exclusively produced by LPET (23, 24). AET reduces photosynthetic O_2 production while also supporting ATP production (23–25). In addition, *Trichodesmium* can perform respiratory protection to wastefully consume organic carbon and intracellular O_2 and protect N_2 fixation (4, 10, 12, 26, 27). O_2 can also physically diffuse between cytoplasm and extracellular environment (Fig. 1A). The direction and rate of O_2 diffusion depend on the difference between intracellular and extracellular O_2 concentration, as well as the O_2 permeability of the cell membrane (ε) which is represented as the relative diffusivity to seawater (28).

In the "dynamic-permeability" model case, the membrane O_2 permeability is assumed to vary diurnally (18). The membrane O_2 permeability is parameterized to increase with intracellular O_2 concentration using a Michaelis-Menten equation (Fig. 1B):

$$\varepsilon = \varepsilon_{\max} \cdot \frac{O_2}{O_2 + k_{O_2}^{\text{diff}}}, \tag{1}$$

where $\varepsilon_{\max}$ is the maximal relative diffusion coefficient of 2.0×10^{-4}, and $k_{O_2}^{\text{diff}}$ (0.213 mol O_2 m^{-3}), a saturating concentration in seawater at 34 PSU salinity and 25°C (29), is the half-saturation constant of O_2 for relative diffusion coefficient.

In addition, to quantitatively assess the physiological roles of DPO_2, we performed another "fixed-permeability" model case with a fixed ε of 1.0×10^{-4}.

Given ε, the rate of O_2 diffusion $\left(T_{O_2,\ \text{mol}\ O_2\ m^{-3}s^{-1}}\right)$ between the intracellular cytoplasm and the extracellular environment is calculated using the scheme proposed by Staal et al. (28) for cylinder-shaped cells:

$$T_{O_2} = \frac{-2 \cdot \Pi \cdot d_{O_2 \cdot L}}{V} \cdot \left\{ \frac{1}{\varepsilon} \cdot \ln\left(\frac{R}{R + L_g}\right) - \ln\left(\frac{R + L_g + L_b}{R + L_g}\right) \right\}^{-1} \cdot \left(O_2^E - O_2\right), \tag{2}$$

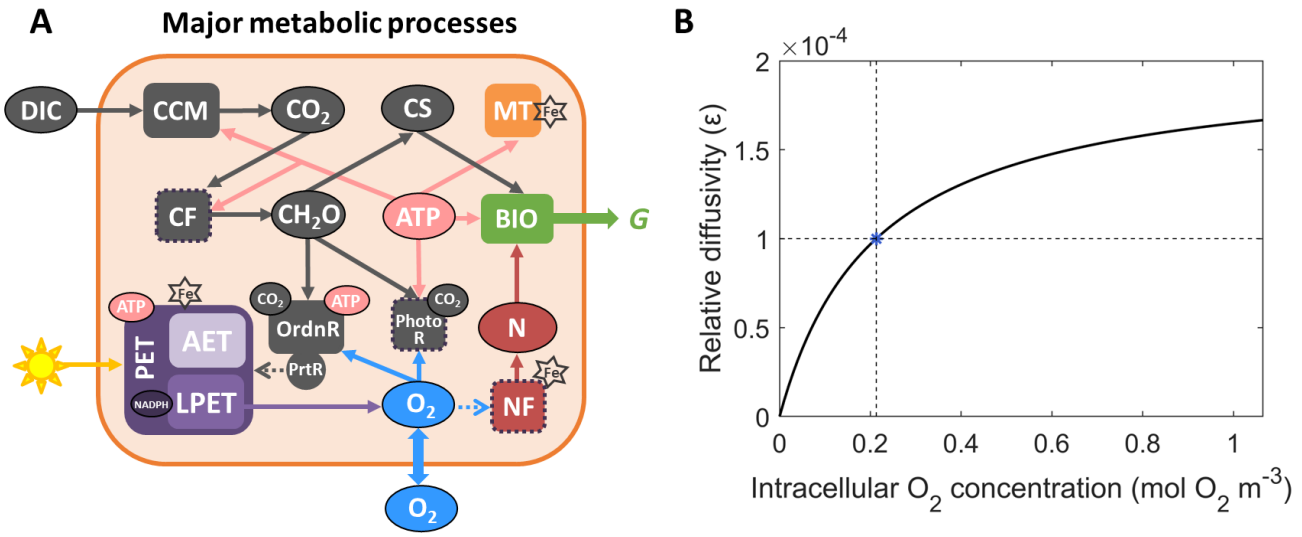

FIG 1 Schematic of the physiological model with potential dynamic O_2 permeability in *Trichodesmium*. (A) Photosynthesis, photorespiration (PhotoR), N_2 fixation, and other key processes are simulated within the *Trichodesmium* trichome. The pentagrams marked Fe-requiring processes, with fundamental intracellular Fe pools shown in Fig. S1A. Dashed arrows represent inhibition effects. CF: carbon fixation; NF: N_2 fixation; PrtR: respiratory protection; OrdnR: ordinary respiration; CH_2O: carbohydrate; CS: carbon skeleton; N: fixed nitrogen; MT: maintenance; BIO: biosynthesis; G: growth rate. (B) The model parameterizes the dynamic O_2 permeability by assuming that the intracellular O_2 concentration regulates the O_2 diffusion coefficient of the cell membrane relative to that of seawater. Blue asterisk denotes the relative diffusivity of the cell membrane at the half-saturating coefficient of intracellular O_2 concentration (0.213 mol O_2 m^{-3}). Note that in the fixed-permeability model case, the reference value of $\varepsilon = 1.0 \times 10^{-4}$ was selected based on observational constraints from prior studies (10, 22).

where d_{O_2} is the O_2 diffusion coefficient in seawater at 34 PSU and 25°C, L (m) and V (m^3) represent the length and the volume of the trichome, R (m) represents the radius of the cytoplasm, L_g (m) denotes the thickness of the cell membrane, L_b (m) denotes the thickness of the boundary layer, and O_2^E refers to the extracellular far-field O_2 concentration.

Photorespiration

Our model additionally represents photorespiration. Photorespiration requires energy using organic carbon and O_2 as substrates (14, 30). The energy usage by photorespiration consequently reduces the energy availability for carbon and N_2 fixation. The maximal photorespiration rate $\left[V_{\mathrm{PR}}^{\max},\ \mathrm{mol\ C\ (mol\ C)^{-1}s^{-1}}\right]$ is computed based on the assumption that ATP produced by PET is fully consumed by photorespiration:

$$V_{\mathrm{PR}}^{\max} = \frac{V_{\mathrm{ATP}}}{q_{\mathrm{PR}}^{\mathrm{ATP}}}, \tag{3}$$

where $q_{\mathrm{PR}}^{\mathrm{ATP}}$ = 7 mol ATP (mol C)$^{-1}$ is the ATP to C ratio in photorespiration (15).

The rate of photorespiration $[V_{\mathrm{PR}},\ \mathrm{mol\ C\ (mol\ C)^{-1}\ s^{-1}}]$ is also regulated by substrates, including intracellular carbohydrate $[CH_2O,\ \mathrm{mol\ C\ (mol\ C)^{-1}}]$ and O_2 $[O_2,\ \mathrm{mol\ O_2\ m^{-3}}]$:

$$V_{PR} = V_{PR}^{max} \cdot \frac{CH_2O}{CH_2O + K_{CH_2O}^{PR}} \cdot \frac{O_2}{O_2 + K_{O_2}^{PR}} \tag{4}$$

where $k_{\mathrm{CH_2O}}^{\mathrm{PR}}$ = 0.4 [mol C (mol C)$^{-1}$] and $k_{\mathrm{O_2}}^{\mathrm{PR}}$ = 1.92 (mol O_2 m^{-3}) are half-saturating coefficients of $CH_2O$and O_2 for photorespiration (Fig. S1B).

The NADPH, ATP, and O_2 consumption rates of photorespiration [V^{PR}_{NADPH}, V^{PR}_{ATP}, $V^{PR}_{O_2}$, mol NADPH (mol C)$^{-1}$ s^{-1}, mol ATP (mol C)$^{-1}$ s^{-1}, and mol O2 (mol C)$^{-1}$ s^{-1} are:

$$V^{PR}_{NADPH} = V_{PR} \cdot q^{NADPH}_{PR}, \quad (5)$$

$$V^{PR}_{ATP} = V_{PR} \cdot q^{ATP}_{PR}, \quad (6)$$

$$V^{PR}_{O_2} = V_{PR} \cdot q^{O_2}_{C,\,PR}, \quad (7)$$

where q^{NADPH}_{PR} = 4 mol NADPH (mol C)$^{-1}$ and $q^{O_2}_{C,\,PR}$ = 3 mol O_2 (mol C)$^{-1}$ are NADPH to C and O_2 to C ratios in photorespiration (15).

N_2 fixation

N_2 fixation was calculated according to previous model schemes (10, 22). N_2 fixation necessitates the utilization of both ATP and NADPH (31, 32). The maximal potential of N_2 fixation rate $\left[V^{max}_{NF}, \text{ mol N (mol C)}^{-1}\text{ s}^{-1}\right]$ occurs when the produced ATP and NADPH from PET are completely consumed by N_2 fixation (10). The rate of N_2 fixation $\left[V_{NF}, \text{ mol N (mol C)}^{-1}\text{ s}^{-1}\right]$(see Supplementary Methods) is limited by the Fe allocated to nitrogenase $\left[Fe_{NF}, \mu\text{mol Fe (mol C)}^{-1}\right]$ (33–35) and can be impended by intracellular O_2, with the rate decreasing upon exposure to O_2 (36).

$$V_{NF} = V^{max}_{NF} \cdot \frac{Fe_{NF}}{Fe_{NF} + k^{NF}_{Fe}} \cdot \left(1 - \frac{O_2}{O_2 + k^{NF}_{O_2}}\right), \quad (8)$$

where k^{NF}_{Fe} [μmol Fe (mol C)$^{-1}$] and $k^{NF}_{O_2}$ (mol O_2 m^{-3}) are half-saturating coefficients of Fe_{NF} and O_2 for N_2 fixation.

Respiratory protection also followed previous model schemes (10, 22). Respiratory protection is a mechanism that involves the wasteful respiration of carbohydrates to reduce intracellular O_2 concentration, thereby supporting N_2 fixation (12). The rate of respiratory protection increases in response to the demand for N_2 fixation, while it decreases as the intracellular O_2 level rises (10, 22).

Carbon fixation

Carbon fixation was computed upon previous models (10, 22) with a minor change by considering photorespiration. Similarly to N_2 fixation, carbon fixation also relies on the availability of both NADPH and ATP (37). To calculate the carbon fixation rate, the total production of NADPH and ATP at each time step is assumed to be promptly and completely utilized by intracellular processes (10, 22), including photorespiration, CCM, carbon fixation, N_2 fixation, and maintenance (10, 22).

Carbohydrates, which are generated through carbon fixation, stimulate the production of carbon skeletons. However, this production is subsequently downregulated due to the accumulation of these carbon skeletons (see Supplemental methods).

Intracellular Fe pools and translocation

This part was conducted based on previous model schemes (10, 22). The total intracellular Fe, which encompasses both metabolism and storage (Fig. S1A), is calculated using a previously established scheme (33). Metabolic Fe includes Fe in photosystems, nitrogenase, maintenance, and buffer (Fig. S1A). Fe utilized by the photosystems and nitrogenase is from the buffer pool (Fig. S1A). The parameterization of synthesis and decomposition rate of photosystems, as well as the synthesis rate of active nitrogenase and its inactivation, is based on a recent model study featuring diurnally dynamic Fe allocation (22).

Considering that DPO_2 may contribute to improving the efficiency of Fe in photosystems and nitrogenase, thus regulating intracellular Fe allocation, model cases were run under various Fe levels for comparison.

Model parameter values

In both fixed and dynamic O_2 permeability model cases, four parameters were optimized to maximize the growth rate of *Trichodesmium* (38). These parameters include the maximal respiratory protection rate (υ_{RP}^{max}), the maximal synthesis $\left(T_{PS_{max}}^{BF}\right)$ and decomposition $\left(T_{BF_{max}}^{PS}\right)$ rates of photosystems, and the maximal synthesis rate $\left(T_{NF_{max}}^{BF}\right)$ of nitrogenase (Table S1). The optimization was performed employing the global optimizer MultiStart in MATLAB.

Other parameters (Table S2) were either adopted from previous studies or tuned to fit the observed growth rates, N_2 fixation rates, and diurnal Fe in photosystems and nitrogenase from a laboratory culture experiment (34). Given that the experiment was conducted under constant light intensity (90 µmol m^{-2} s^{-1}), we adopted the same light intensity as DPO_2. After tuning model parameters (Table S2), the modeled growth rates (0.28 and 0.45 d^{-1} under low and high Fe, respectively) were well aligned with the observations (Table S4). Moreover, the model reproduced diurnal patterns of photosystem and nitrogenase (under low and high Fe, for photosystem Fe, R^2 = 0.13 and 0.90, respectively; for nitrogenase Fe, R^2 = 0.60 and 0.80, respectively) (Fig. S2). The low R^2 value for photosystem Fe under the low Fe condition reflects substantial natural variability in *Trichodesmium* physiology, generally compounded by nonlinear environmental interactions (34, 35). While limited observational points (5 samples during the light period) were used for constraints, the model still captured key diurnal dynamics (Fig. S2), with R^2 values expected to improve through higher-resolution sampling. In addition, the reliability index (RI) (Equation 9) (39, 40) was calculated to further evaluate the performance of the model compared to observations (under low and high Fe, for photosystem Fe, RI = 1.04 and 1.02, respectively; for nitrogenase Fe, RI = 1.14 and 1.01, respectively). These RI levels close to 1.0 indicate strong consistency between observations and model results, supporting the robustness of our model (39, 40).

$$\mathrm{RI} = \exp\left(\sqrt{\frac{1}{n}\sum_{i=1}^{n}\left(\ln\frac{\mathrm{Observation}_i}{\mathrm{Model}_i}\right)^2}\right), \tag{9}$$

where Observation and Model are observations and model results, respectively; n is the number of observational data points.

Note that the constant light intensity was only used when tuning model parameters. All the model results presented in the following were simulated with dynamic light intensity using a sine function over a 12 hour light period (41).

RESULTS

Simulated growth rate, carbon and N_2 fixation rates, and O_2 concentration

Similar to a previous model study (22), the simulations encompassed 10 Fe′ levels (20–1,800 pM) to approximately represent the *Trichodesmium* Fe quota of 10–1,000 µmol Fe (mol C)$^{-1}$, a range observed in field *Trichodesmium* samples (33). Our model showed a positive correlation between Fe concentration and both N_2 fixation and growth rates (Fig. S3), consistent with trends from previous culturing experiments of *Trichodesmium* (35). In addition, model results exhibited that the influence of DPO_2 on promoting growth rates decreased from 78% to 33% as Fe concentration increased (Fig. S3), indicating that the physiological benefits of DPO_2 in *Trichodesmium* were more pronounced under low Fe conditions. In the following, we focused on analyzing the model results at two levels of dissolved inorganic Fe (40 pM and 1,250 pM) that were set

in the laboratory experiments (34). Under these two Fe levels, DPO_2 promoted modeled growth rates of *Trichodesmium* by 61% and 30%, respectively.

Our results revealed that while the dynamic-permeability case exhibited higher growth rates than the fixed-permeability case under both Fe conditions, the gross carbon fixation rates in the dynamic-permeability case were even lower (Fig. 2). This implies that dynamic O_2 permeability led to an improvement in carbon use efficiency of *Trichodesmium*, defined here as the ratio of net to gross carbon production (Fig. 2). The decrease in the requirement for carbon fixation and the increase in carbon use efficiency is attributed to the lowered photorespiration and the downregulated requirement of respiratory protection (see Discussion) (Fig. 2). Furthermore, our simulation results aligned with previous studies (22, 42, 43), demonstrating higher carbon use efficiency under higher Fe conditions.

DPO_2 benefits modeled *Trichodesmium* via modulating carbon and N_2 fixation rates and intracellular O_2 levels, with the physiological roles of DPO_2 differing in two periods (Fig. 3). We first analyzed results under low-Fe conditions.

During the early period, compared to the fixed-permeability case, the carbon fixation rate in the dynamic-Fe case was slightly lower with a decreasing pattern (approximately 1–4 h) (Fig. 3A). This indicates that DPO_2 could lower the requirement for carbon storage. In addition, lower intracellular O_2 level in the dynamic-permeability case (Fig. 3E and G) reduced the carbon consumption by photorespiration (see Discussion).

During the low-O_2 window, the N_2 fixation rate in the dynamic-permeability case was higher (Fig. 3C). A wider low-O_2 window was presented in the dynamic-permeability case (Fig. 3E), suggesting DPO_2 could reduce the stress from O_2 on N_2 fixation (see Discussion).

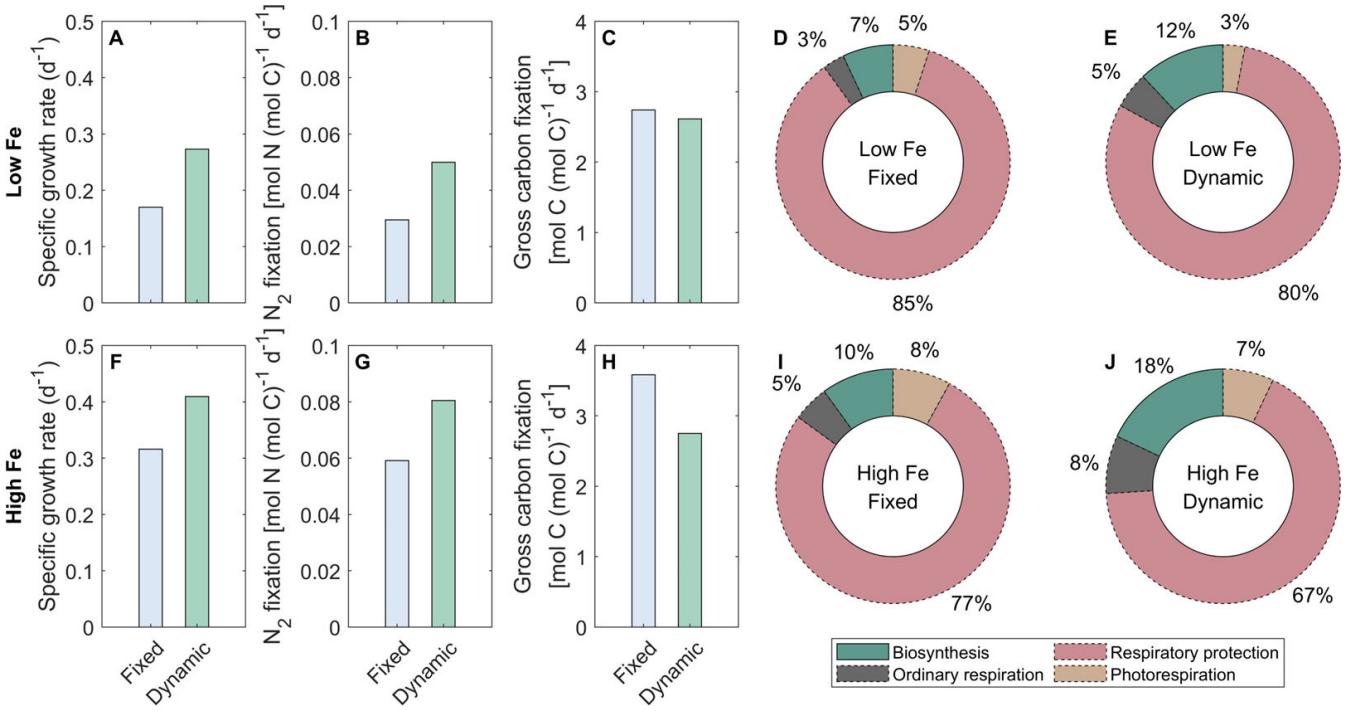

FIG 2 Modeled daily-integrated results of *Trichodesmium*. The model is simulated with diurnally fixed and dynamic O_2 permeability of the cell membrane under low-Fe (40 pM) and high-Fe (1,250 pM) conditions. Model results include growth rates (A, F), N_2 fixation rates (B, G), and gross carbon fixation rates (C, H).The number in the inner circle represents the daily-integrated gross carbon fixation rate (mol C [mol C]$^{-1}$ d^{-1}). The fixed carbon is allocated to photorespiration, respiratory protection, ordinary respiration, and biosynthesis. Carbon use efficiency: the fraction of gross fixed carbon allocated to biosynthesis, which is highlighted using solid lines (D, E, I, and J).

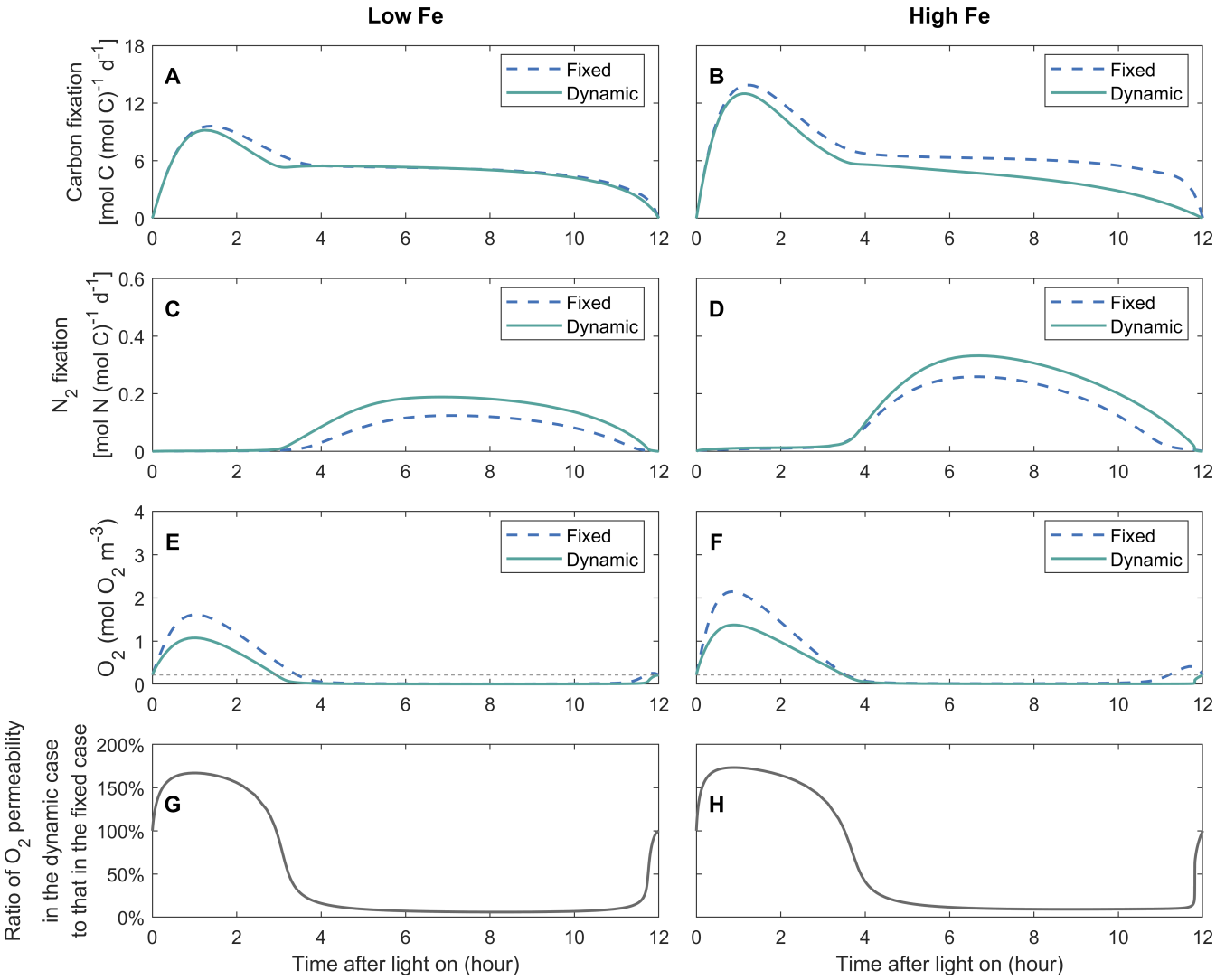

FIG 3 Simulated instantaneous rates of gross carbon fixation and N_2 fixation, intracellular O_2 concentrations, and O_2 permeability of the cell membrane during the light period. The O_2 permeability is shown as the ratio of its values in the dynamic-permeability case to those in the fixed-permeability case. The model is simulated with diurnally fixed and dynamic O_2 permeability of the cell membrane under low-Fe (40 pM) (A, C, E, and G) and high-Fe (1250 pM) (B, D, F, and H) conditions. The thin black dashed lines represent the ambient far-field O_2 concentration.

Under the high-Fe condition, diurnal patterns of modeled carbon and N_2 fixation rates and intracellular concentrations were similar to those under the low-Fe condition, but at slightly higher levels (Fig. 3).

Simulated diurnal intracellular O_2 fluxes

The physiological functions of DPO_2 in regulating intracellular O_2 fluxes varied diurnally. During the early daytime (approximately 0–3 h of the light period), the daily-integrated net O_2 production rate by PET was slightly lower compared to the dynamic-permeability case under low Fe (Fig. 4A), with a more pronounced difference under high Fe (Fig. 4B) (see Discussion). Intracellular O_2 diffused out of the cell cytoplasm (Fig. 4C and D) due to the high intracellular O_2 concentration (Fig. 3E and F), induced by the high net O_2 production rate of PET (Fig. 4A and B). The intracellular O_2 concentration in the dynamic-permeability case was lower than that in the fixed-permeability case (Fig. 3E and F), while the physical diffusion rates of O_2 in both cases were similar (Fig. 3C and D). This can be attributed to the higher O_2 permeability of the cell membrane in

the dynamic-permeability case (Fig. 3G and H), which facilitated quick intracellular O_2 diffusion into the extracellular environment.

In addition, high intracellular O_2 concentrations during this period stimulated photorespiration (Fig. 4E and F). The lower photorespiration rates in the dynamic-permeability case (Fig. 4E and F) were attributed to reduced intracellular O_2 concentration (Fig. 3E and F). Therefore, DPO_2 has the potential to alleviate the stress caused by photorespiration, particularly during the early daytime when the net O_2 production rate is high.

In the following light period, the intracellular low-O_2 window was created (Fig. 3E and F) due to the downregulation of the net O_2 production by PET (Fig. 4A and B) and the high O_2 consumption by respiratory protection (Fig. 4G and H) (10), allowing the occurrence of N_2 fixation. Extracellular O_2 diffused into the cytoplasm (Fig. 4C and D), which was slowed down by the lowered O_2 permeability in the dynamic-permeability case (Fig. 3G and H). Therefore, DPO_2 saved organic carbon required by respiratory protection (Fig. 4G and H) to maintain low O_2 levels in *Trichodesmium* (Fig. 3). In both the dynamic- and fixed-permeability cases, the photorespiration rate approached zero during this period (Fig. 4E and F), indicating that the creation of the low-O_2 window also helped to mitigate O_2-induced stresses on photosynthesis.

DISCUSSION

In this study, we developed a physiological model of *Trichodesmium* trichome to quantitatively investigate the impact of photorespiration and the physiological advantages of DPO_2 (Fig. 1). Intracellular O_2 management such as respiratory protection was considered, with the temporal segregation between photosynthesis and N_2 fixation formed and the low-O_2 window created (Fig. 3). These were in line with previous model studies and observations (4, 9, 10, 12, 22). The model results demonstrate that DPO_2 enhanced *Trichodesmium* N_2 fixation and growth rates (Fig. 2, 3, and 5 and S3) by decreasing photorespiration and respiratory protection and increasing carbon and Fe use efficiency.

Dynamic O_2 permeability lowers photorespiration

In the model case when the O_2 permeability was fixed, 5% and 8% of the daily-integrated gross fixed carbon were consumed by photorespiration under low-Fe and high-Fe conditions, respectively (Fig. 2, 4E, and F), which is comparable to the fractions allocated to biomass synthesis (Fig. 2). These low proportions of photorespiration seem reasonable in *Trichodesmium*, which operates carbon concentrating mechanisms (44) to enhance carbon fixation and minimize the oxygenation reaction (i.e., photorespiration) by RuBisCO (14). After implementing DPO_2, modeled photorespiration rates were reduced by 42% and 35% in the dynamic-permeability case, respectively (Fig. 2, 4E, F and 5), resulting in a corresponding increase in gross fixed carbon allocated to biomass synthesis (Fig. 2). This was also found in the model experiments under constant light intensity (Fig. S4B). Further model experiments demonstrated that substituting the photorespiration rates in the dynamic-permeability case with those derived from the fixed-permeability case led to a reduction in *Trichodesmium* growth rates by 10% and 9% under low- and high-Fe conditions, respectively. These findings indicate that DPO_2 has the potential to improve carbon use efficiency and growth rate of *Trichodesmium* by reducing its photorespiration.

The reduction of photorespiration in the dynamic-permeability case (Fig. 4E and F) was partially attributed to the increased O_2 permeability during the early daytime (Fig. 3G, H, and 5), facilitating the diffusion of intracellular O_2 into the extracellular environment and resulting in lower intracellular O_2 concentration (Fig. 3E and F).

In addition, DPO_2 also resulted in a decrease in photosynthesis and O_2 production evolution during the early light period (Fig. 3A, B and 4A and B), contributing to reducing the intracellular O_2 concentration (Fig. 3E and F) and photorespiration rate (Fig. 4E, F, and 5). This can be attributed to the reduced need for respiratory protection during the

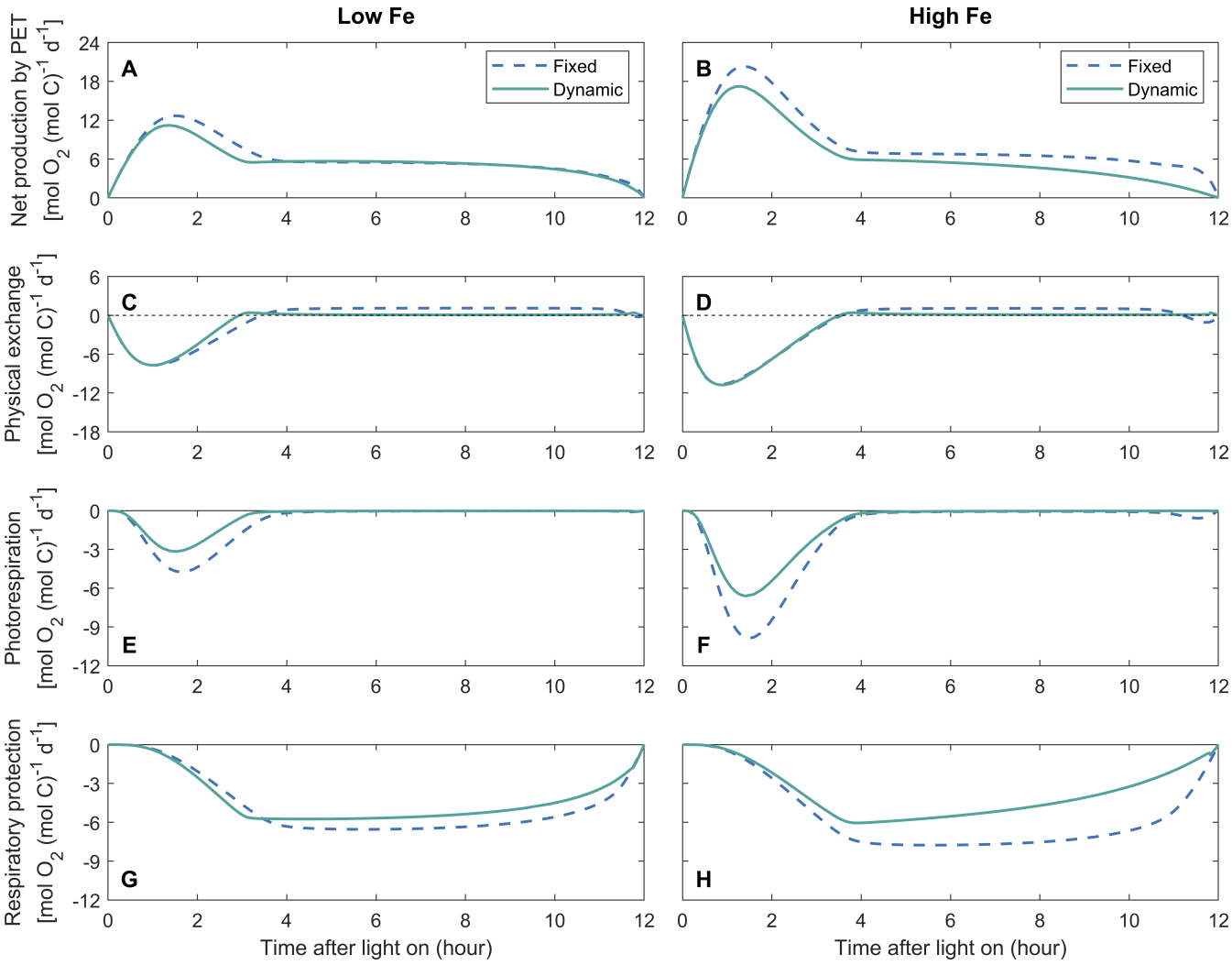

FIG 4 Simulated diurnal intracellular O_2 fluxes. O_2 fluxes include net production by photosynthetic electron transfer (PET), physical exchange between intracellular and extracellular environments, O_2 consumption by photorespiration, and respiratory protection (negative values). Positive physical O_2 exchange represents O_2 flux into cells. The model is simulated with diurnally fixed or dynamic O_2 permeability of the cell membrane under low-Fe (40 pM) (A, C, E, and G) and high-Fe (1,250 pM) (B, D, F, and H) conditions.

low-O_2 window (Fig. 4G, H, and 5), thereby downregulating the requirement for carbon fixation (Fig. 3A, B , and 5) and Fe allocated to photosystems (Fig. S5A and B) during the early daytime (discussed later).

Laboratory experiments on *Trichodesmium* have shown that light-dependent O_2 uptake (which involves photorespiration as well as Mehler reaction and potentially flv-mediated O_2 uptake) can indeed be dynamically regulated by external O_2 and CO_2 concentrations: When external O_2 levels in the media were decreased or increased, light-dependent O_2 uptake changed proportionally within minutes in a reversible fashion (9). Another recent culture study of *Trichodesmium* also proposed a decrease in photorespiration under low-O_2 conditions (< 0.213 mol O_2 m^{-3}), although it was not quantified (16). In addition, the rate of light-dependent O_2 consumption has been shown to increase with an increase in CO_2 concentration in the medium (45).

A previous study proposed that photorespiration could serve as a mechanism to protect nitrogenase and N_2 fixation by consuming the O_2 produced by LPET, which, however, lacked support from observations or model simulations (46). In our model study, photorespiration primarily occurred during the early light period (Fig. 4E and F), when it was stimulated by high intracellular O_2 concentrations (Fig. 3E and F), while there

was minimal photorespiration during the low-O_2 window when N_2 fixation predominantly occurred (Fig. 4E and F). This low photorespiration could occur when high levels of respiratory protection depleted O_2 and produced CO_2 in *Trichodesmium* (Fig. 4G and H) (14), although the intracellular CO_2 concentration was not simulated in our study. In other words, this suggests that respiratory protection played a major role in lowering the intracellular O_2 level for N_2 fixation, while photorespiration may only have a limited contribution.

Dynamic O_2 permeability reduces the requirement for respiratory protection

In the fixed-permeability case, 85% and 77% of the gross fixed carbon were allocated to respiratory protection to consume intracellular O_2 and create the low-O_2 window for N_2 fixation under low-Fe and high-Fe conditions, respectively (Fig. 2, 4G, and H). These percentages were generally consistent with previous model studies that adopted fixed O_2 permeability of the cell membrane over the light period (10, 12, 22) or even other N_2 fixers (47, 48). In comparison, in the dynamic-permeability case, the fractions of gross fixed carbon allocated to respiratory protection were reduced to 80% and 67% under low-Fe and high-Fe conditions, respectively (Fig. 2, 4G, and H). This reduction in respiratory protection was primarily attributed to the low-O_2 permeability in the dynamic-permeability case, which decreased the diffusion rate of extracellular O_2 into the cytoplasm (Fig. 4C, D, and 5). As a result, the intracellular stress on N_2 fixation caused by extracellular O_2 was basically relieved. Consequently, lower rates of O_2-consuming respiratory protection (Fig. 4G, H, and 5) were required to create and maintain lower intracellular O_2 concentrations (Fig. 3E and F and S4A, B), thereby supporting higher N_2 fixation rates in the dynamic-permeability case (Fig. 3A, B, and 5).

Previous model studies have proposed that respiratory protection is a crucial strategy for managing the intracellular O_2 level and creating the low-O_2 condition for N_2 fixation in *Trichodesmium* and other N_2-fixing cyanobacteria, such as *Crocosphaera* (4, 10, 48–50). Consistent with the previous study, our study demonstrated that respiratory protection respired major gross fixed carbon to consume intracellular O_2, resulting in a high indirect cost for N_2 fixation. This is also supported by observations of high daily-integrated gross fixed C:N ratios (e.g., references 30–50), even when Fe is replete (4, 9, 51, 52). Lowering carbon demand may allow this high ratio of carbon to be channeled into growth, thus increasing ecological competitiveness. Therefore, *Trichodesmium* might develop several strategies to reduce the requirement for respiratory protection and promote the carbon use efficiency, such as the dynamic Fe allocation, of which the function was quantified in a recent model study (22). On top of that, our study highlights the role of DPO_2 in lowering respiratory protection and alleviating the stress from O_2 on N_2 fixation in *Trichodesmium*.

Dynamic O_2 permeability improves Fe use efficiency

The dynamic-permeability model case exhibited higher rates of N_2 fixation and growth compared to the fixed-permeability case under both low and high Fe levels (Fig. 2, 3 and 5 and S3), thereby promoting Fe use efficiency by 69% and 36%, respectively (Fig. 6).

The simulated diurnal patterns of Fe in both photosystems and nitrogenase suggest that DPO_2 could regulate intracellular Fe allocation (Fig. S5). Specifically, in the dynamic-permeability case, less Fe was allocated to photosystems during the light period compared to the fixed-permeability case (Fig. S5A and B). This can be attributed to two main reasons. First, the reduction in photorespiration allowed for the saving of energy and NADPH, which then can be utilized by carbon fixation. Second, the downregulation of respiratory protection decreased the demand for carbon fixation and storage in early daytime (Fig. 3 and 5). In addition, decreased respiratory protection mitigated the inhibition on photosynthetic electron transfer (4). Consequently, the Fe demand of photosystems was reduced in the dynamic-permeability case (Fig. 5 and S5A and B). The saved Fe from photosystems could then be allocated to (active) nitrogenase (Fig. 5 and S5C to F), enhancing N_2 fixation (Fig. 3C, D, and 5).

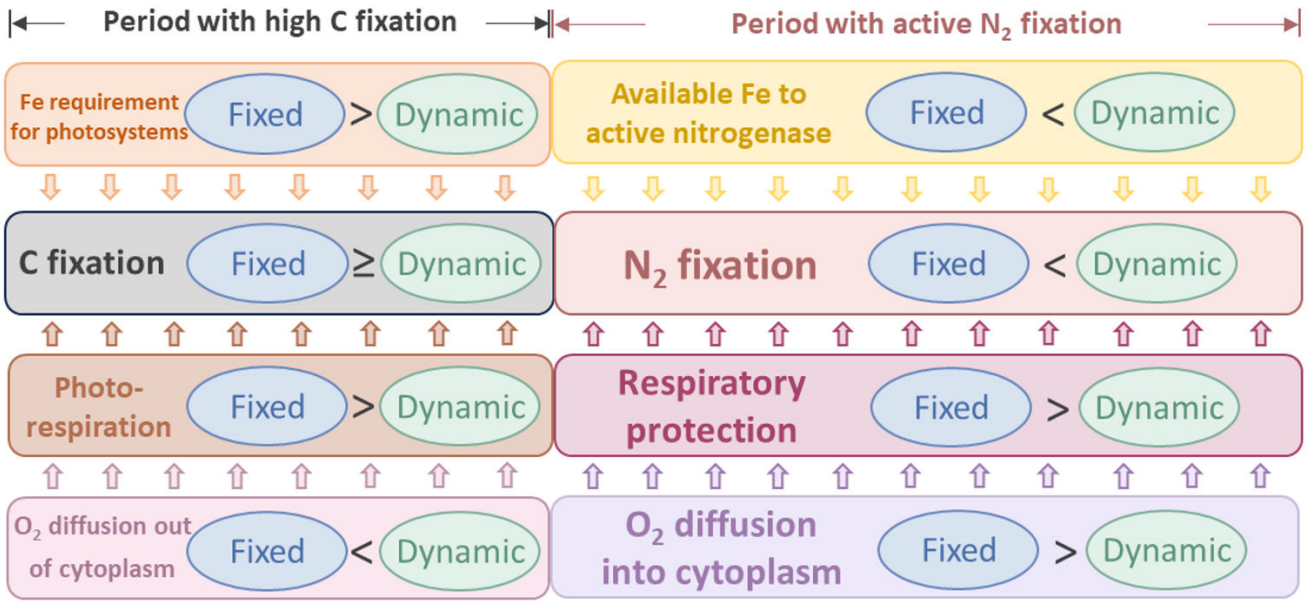

FIG 5 Schematic diagram illustrating diurnally fixed and dynamic O_2 permeability of the cell membrane. Dynamic O_2 permeability can reduce photorespiration and the requirement for respiratory protection. In addition, it can promote carbon and iron use efficiency. Arrows between boxes represent the influence on carbon fixation and N_2 fixation.

In conclusion, our model study highlights two main potential mechanisms explaining the benefits of dynamic O_2 permeability to N_2 fixation and growth in *Trichodesmium*, which include the reduced photorespiration and decreased requirement for respiratory protection (Fig. 5). This can improve carbon and Fe use efficiency (Fig. 5 and 6), as well as N_2 fixation and growth rates of *Trichodesmium*, especially under low Fe. Therefore,

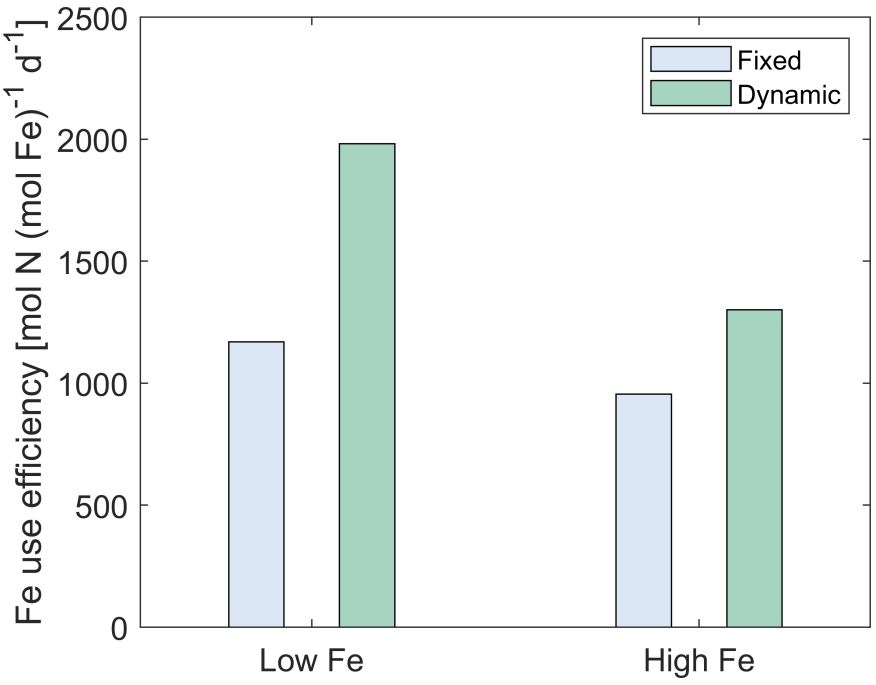

FIG 6 Modeled results of Fe use efficiency in *Trichodesmium*. The model is simulated with diurnally fixed and dynamic O_2 permeability of the cell membrane under low-Fe (40 pM) and high-Fe (1,250 pM) conditions. Fe use efficiency: the ratio of the daily-integrated N_2 fixation rate to intracellular metabolic Fe.

this strategy potentially alleviates Fe limitation, helping *Trichodesmium* survive in the oligotrophic open ocean.

As phototrophic phytoplankton, *Trichodesmium* primarily inhabits the upper euphotic zone (53), where dissolved O_2 concentrations typically approach saturation (54). Baseline simulations were therefore set to the external O_2 concentration at 0.213 mol m^{-3}, which represents the saturation level for a typical upper ocean (salinity: 34 PSU; temperature: 25 °C) (29). Under specific circumstances, such as in the center of the microenvironment within *Trichodesmium* colonies, however, O_2 concentrations have been observed to be up to 200% saturation, especially under high light intensities (55). Model experiments across a range of O_2 concentrations (Fig. S6) show that photorespiration and nitrogenase inactivation become more intense and highlight that the benefits of dynamic O_2 permeability are amplified at elevated external O_2 levels. This suggests that dynamic permeability may be particularly important in *Trichodesmium* colonies at the sea surface subjected to high light intensities.

It should be noted that in our model, variations in the O_2 permeability of the *Trichodesmium* cell membrane were assumed to occur instantly in response to intracellular O_2 levels. However, further investigation is required to explore the timescale and the efficiency of redistributing hopanoid lipids in the cell membrane of *Trichodesmium*, which regulates the O_2 permeability. This will provide a more comprehensive understanding of the physiological benefits associated with DPO_2 in *Trichodesmium*. Further sensitivity model experiments of the maximal relative diffusion coefficient demonstrate that a proper range of variation/modulation in dynamic O_2 permeability is necessary for physiological benefits on N_2 fixation and growth in *Trichodesmium* (Fig. S7).

Broader context: is dynamic O_2 permeability a common strategy in marine cyanobacterial diazotrophs?

The gene for the synthesis of hopanoids (the squalene-hopene cyclase gene, *shc*) was reported to be present in UCYN-A (nitroplast), UCYN-B (*Crocosphaera*), and UCYN-C (*Cyanothece*) (18, 56–61), suggesting their potential in dynamically regulating the membrane permeability to O_2 (Table 1). Hopanoids are known to decrease membrane O_2 permeability, protecting intracellular processes such as nitrogenase activity (18). However, direct evidence of diel variation in hopanoid production or dynamic changes in membrane lipid composition remains limited in marine diazotrophs.

A recent transcriptomic study (62) reveals diurnal cycling of gene expression in *Crocosphaera*, including genes related to photosynthesis and N_2 fixation, suggesting that membrane lipid composition may be dynamically regulated over diel cycles. Similarly, in non-diazotrophic cyanobacteria like *Synechocystis* sp. PCC 6803, diel light-dark cycles significantly influence fatty acid synthesis and membrane lipid turnover (63). Beyond cyanobacteria, studies in plants show that membrane lipid turnover can occur on timescales as short as 2 hours (64), suggesting that dynamic regulation of membrane lipids is a widespread strategy across diverse organisms. Together, these findings support the plausibility of DPO_2 as a physiological strategy in marine diazotrophs.

While the diel rhythms of photosynthesis and N_2 fixation in these marine non-heterocyst-forming diazotrophic cyanobacteria may differ from *Trichodesmium* (65, 66), it

TABLE 1 Summary of indications from literature for dynamic O_2 permeability with potential benefits in some marine cyanobacterial diazotrophs

Diazotroph	Indications/potential for dynamic O_2 permeability	References
Trichodesmium	Yes	This study and (18)
UCYN-A (nitroplast)	Possible	(58)
UCYN-B (*Crocosphaera*)	Yes	(56)
UCYN-C (*Cyanothece*)	Yes	(56)
Diazotroph-diatom association (DDA)	No	(18)

is possible that the proposed physiological advantages of DPO_2 may apply to these diazotrophs.

The physiological roles of DPO_2 in improving the carbon and Fe use efficiency in some marine diazotrophs were similar to those of the dynamic Fe allocation (22). This suggests that dynamic regulation of membrane permeability can facilitate N_2 fixation and the growth of these diazotrophs in a manner similar to dynamic regulation of physiological processes, including temporal segregation (65, 67) and potential rapid mode switching (68) between photosynthesis and N_2 fixation. The in-depth controlling mechanisms of dynamic strategies guarantee further research.

UCYN-A

The genome of UCYN-A (or nitroplast) (60) is highly reduced and lacks genes for O_2-producing photosystem II (69), suggesting a potential reduction in O_2-induced stresses and photorespiration. A previous study demonstrated coordination between the expression of the shc gene and the *nifH* gene (encoding nitrogenase) in UCYN-A (56). This indicates that UCYN-A may regulate membrane permeability to O_2 dynamically, lowering intracellular O_2 levels and protecting nitrogenase activity by mitigating O_2 diffusion from the O_2-producing haptophyte algal host cell and the ambient environment into the cytoplasm during active N_2 fixation. In addition, the low transcription level of the cytochrome c oxidase *coxA* gene in UCYN-A during the light period (26, 56) indicates a reduced requirement for respiratory protection. According to insights from this study, such dynamic regulation could enhance carbon and Fe use efficiency in UCYN-A.

UCYN-B and UCYN-C

Both UCYN-B (*Crocosphaera*) and UCYN-C (*Cyanothece*) conduct photosynthesis during the light period and N_2 fixation at night (56, 70–72). Transcriptomic analysis has shown that the shc gene in UCYN-B and UCYN-C reached its peak expression just before the increase in the nifH gene expression level (56). This observation suggests that UCYN-B and UCYN-C may produce hopanoids to protect N_2 fixation from O_2 diffusing from the external environment during the dark period, therefore reducing the level of respiratory protection required to safeguard nitrogenase and support N_2 fixation (48, 49). In addition, lower expression of the shc gene during the daytime in UCYN-B and UCYN-C (56) might result in higher O_2 permeability, facilitating the diffusion of photosynthetically produced O_2 out of the cell and thus reducing photorespiration. These mechanisms, as proposed in this study, would lead to elevated carbon and Fe use efficiency. In addition, these organisms have heterogeneous rates of N_2 fixation (i.e., some cells fix N_2 and others do not) (73), and thus, the most effective DPO_2 would also be heterogeneous across their population. Furthermore, the presence of hopanoid rafts in UCYN-B (74) suggests that hopanoid may be redistributed within the membrane to dynamically modulate O_2 permeability (20).

DDAs

Heterocyst-forming diazotrophs (diatom-diazotroph assemblage, DDA) lack the shc gene responsible for hopanoid synthesis (18). This indicates that DPO_2 may not be necessary in DDA. Instead, the heterocyst uses glycolipids to form a barrier against extracellular O_2 (75, 76), seemingly providing sufficient protection for nitrogenase activity and reducing Fe requirements compared to non-heterocyst-forming cyanobacterial diazotrophs (77). Similarly, the absence of the shc gene in non-diazotrophic cyanobacteria such as *Prochlorococcus* and *Synechococcus* (18) further supports the idea that DPO_2 is one of the evolved strategies of diazotrophs when facing O_2 stress on N_2 fixation.

Conclusions

We investigated how dynamic cell permeability to O_2 (DPO_2) in *Trichodesmium* trichomes may enhance N_2 fixation and growth rates, taking into account the effect of photorespiration. Our model shows that DPO_2 reduces photorespiration, especially during the early daytime, lowering the requirement for respiratory protection, facilitating the formation of the low-O_2 intracellular condition for N_2 fixation, and improving carbon use efficiency. Moreover, DPO_2 in *Trichodesmium* may impact the diurnal allocation of the intracellular Fe, ultimately promoting the Fe use efficiency. Fragmental evidence for DPO_2 is reported in other marine diazotrophs, suggesting that DPO_2 is a common strategy adopted by marine diazotrophs. The model framework presented in our study could also be used to explore other physiological mechanisms that control N_2 fixation, such as light and Fe colimitation. It can also be incorporated into biogeochemical models to enhance their predictive capabilities in the ecophysiology of marine diazotrophs.

ACKNOWLEDGMENTS

This project is partly supported by the National Natural Science Foundation of China (42076153 and 42376140 to YWL), China Scholarship Council, and MEL PhD Fellowship to WL. This work was supported by a grant from the Simons Foundation (LS-ECIA-MEE-00001549, Inomura). O.P. is supported by GACR 23-06593S and by OP JAK Photomachines. M.E. is supported by GACR GA24-12396S and by OP JAK project Photomachines.

W.L. and Y.W.L. originated the concept for the study. W.L. designed the numerical model. W.L. coded the initial version of the model and performed numerical modeling. W.L., K.I., O.P., M.E., and Y.W.L. analyzed the results and improved the numerical model. W.L. wrote the first draft of the manuscript, and all coauthors revised the manuscript.

AUTHOR AFFILIATIONS

[1]State Key Laboratory of Marine Environmental Science and College of Ocean and Earth Sciences, Xiamen University, Xiamen, China
[2]Centre Algatech, Institute of Microbiology of the Czech Academy of Sciences, Třeboň, Czech Republic
[3]Institute for Advanced Study, Shenzhen University, Shenzhen, China
[4]Graduate School of Oceanography, University of Rhode Island, Narragansett, Rhode Island, USA

AUTHOR ORCIDs

Weicheng Luo http://orcid.org/0000-0002-4377-2030
Keisuke Inomura http://orcid.org/0000-0001-9232-7032
Ondřej Prášil http://orcid.org/0000-0002-0012-4359
Meri Eichner http://orcid.org/0000-0001-6106-7880
Ya-Wei Luo http://orcid.org/0000-0001-6106-7901

AUTHOR CONTRIBUTIONS

Weicheng Luo, Conceptualization, Data curation, Formal analysis, Investigation, Methodology, Software, Validation, Visualization, Writing – original draft, Writing – review and editing | Keisuke Inomura, Formal analysis, Funding acquisition, Methodology, Validation, Visualization, Writing – review and editing | Ondřej Prášil, Formal analysis, Funding acquisition, Methodology, Validation, Visualization, Writing – review and editing | Meri Eichner, Formal analysis, Funding acquisition, Methodology, Validation, Visualization, Writing – review and editing | Ya-Wei Luo, Conceptualization, Formal analysis, Funding acquisition, Methodology, Validation, Visualization, Writing – review and editing

DATA AVAILABILITY

All data, code, and materials used in this study are available from the corresponding author upon reasonable request. The code is freely available in figshare (https://doi.org/10.6084/m9.figshare.28829270).

ADDITIONAL FILES

The following material is available online.

Supplemental Material

Supplemental material (Spectrum00453-25-S0001.pdf). Supplemental methods, Tables S1 to S4, and Fig. S1 to S7.

Open Peer Review

PEER REVIEW HISTORY (review-history.pdf). An accounting of the reviewer comments and feedback.

REFERENCES

1. Capone DG, Zehr JP, Paerl HW, Bergman B, Carpenter EJ. 1997. *Trichodesmium* , a globally significant marine cyanobacterium . Science 276:1221–1229. https://doi.org/10.1126/science.276.5316.1221
2. Capone DG, Burns JA, Montoya JP, Subramaniam A, Mahaffey C, Gunderson T, Michaels AF, Carpenter EJ. 2005. Nitrogen fixation by *Trichodesmium* spp.: an important source of new nitrogen to the tropical and subtropical North Atlantic Ocean . Global Biogeochem Cycles 19. https://doi.org/10.1029/2004GB002331
3. Reynolds SE, Mather RL, Wolff GA, Williams RG, Landolfi A, Sanders R, Woodward EMS. 2007. How widespread and important is N_2 fixation in the North Atlantic Ocean? . Global Biogeochem Cycles 21:GB4015. https://doi.org/10.1029/2006GB002886
4. Berman-Frank I, Lundgren P, Chen YB, Küpper H, Kolber Z, Bergman B, Falkowski P. 2001. Segregation of nitrogen fixation and oxygenic photosynthesis in the marine cyanobacterium *Trichodesmium*. Science 294:1534–1537. https://doi.org/10.1126/science.1064082
5. Staal M, Rabouille S, Stal LJ. 2007. On the role of oxygen for nitrogen fixation in the marine cyanobacterium *Trichodesmium* sp. Environ Microbiol 9:727–736. https://doi.org/10.1111/j.1462-2920.2006.01195.x
6. Wang ZC, Burns A, Watt GD. 1985. Complex formation and O_2 sensitivity of *Azotobacter vinelandii* nitrogenase and its component proteins. Biochemistry 24:214–221. https://doi.org/10.1021/bi00322a031
7. Held NA, Waterbury JB, Webb EA, Kellogg RM, McIlvin MR, Jakuba M, Valois FW, Moran DM, Sutherland KM, Saito MA. 2022. Dynamic diel proteome and daytime nitrogenase activity supports buoyancy in the cyanobacterium *Trichodesmium*. Nat Microbiol 7:300–311. https://doi.org/10.1038/s41564-021-01028-1
8. Hania A, López-Adams R, Prášll O, Eichner M. 2023. Protection of nitrogenase from photosynthetic O_2 evolution in *Trichodesmium*: methodological pitfalls and advances over 30 years of research. Photosynthetica 61:58–72. https://doi.org/10.32615/ps.2023.007
9. Finzi-Hart JA, Pett-Ridge J, Weber PK, Popa R, Fallon SJ, Gunderson T, Hutcheon ID, Nealson KH, Capone DG. 2009. Fixation and fate of C and N in the cyanobacterium *Trichodesmium* using nanometer-scale secondary ion mass spectrometry. Proc Natl Acad Sci USA 106:6345–6350. https://doi.org/10.1073/pnas.0810547106
10. Luo W, Inomura K, Zhang H, Luo YW. 2022. N2 fixation in *Trichodesmium* does not require spatial segregation from photosynthesis mSystems 7:e00538–22. https://doi.org/10.1128/msystems.00538-22
11. Nicholson DP, Stanley RHR, Doney SC. 2018. A phytoplankton model for the allocation of gross photosynthetic energy including the trade - offs of diazotrophy. JGR Biogeosciences 123:1796–1816. https://doi.org/10.1029/2017JG004263
12. Inomura K, Wilson ST, Deutsch C. 2019. Mechanistic model for the coexistence of nitrogen fixation and photosynthesis in marine *Trichodesmium* mSystems 4:e00210-19. https://doi.org/10.1128/mSystems.00210-19
13. Eichner M, Thoms S, Rost B, Mohr W, Ahmerkamp S, Ploug H, Kuypers MMM, de Beer D. 2019. N_2 fixation in free-floating filaments of *Trichodesmium* is higher than in transiently suboxic colony microenvironments. New Phytol 222:852–863. https://doi.org/10.1111/nph.15621
14. Moroney JV, Jungnick N, DiMario RJ, Longstreth DJ. 2013. Photorespiration and carbon concentrating mechanisms: two adaptations to high O_2, low CO_2 conditions. Photosynth Res 117:121–131. https://doi.org/10.1007/s11120-013-9865-7
15. Bauwe H, Hagemann M, Fernie AR. 2010. Photorespiration: players, partners and origin. Trends Plant Sci 15:330–336. https://doi.org/10.1016/j.tplants.2010.03.006
16. Li H, Gao K. 2023. Deoxygenation enhances photosynthetic performance and increases N_2 fixation in the marine cyanobacterium *Trichodesmium* under elevated pCO2. Front Microbiol 14:1102909. https://doi.org/10.3389/fmicb.2023.1102909
17. Eisenhut M, Roell MS, Weber APM. 2019. Mechanistic understanding of photorespiration paves the way to a new green revolution. New Phytol 223:1762–1769. https://doi.org/10.1111/nph.15872
18. Cornejo-Castillo FM, Zehr JP. 2019. Hopanoid lipids may facilitate aerobic nitrogen fixation in the ocean. Proc Natl Acad Sci USA 116:18269–18271. https://doi.org/10.1073/pnas.1908165116
19. Poger D, Mark AE. 2013. The relative effect of sterols and hopanoids on lipid bilayers: when comparable is not identical. J Phys Chem B 117:16129–16140. https://doi.org/10.1021/jp409748d
20. Belin BJ, Busset N, Giraud E, Molinaro A, Silipo A, Newman DK. 2018. Hopanoid lipids: from membranes to plant-bacteria interactions. Nat Rev Microbiol 16:304–315. https://doi.org/10.1038/nrmicro.2017.173
21. Frischkorn KR, Haley ST, Dyhrman ST. 2018. Coordinated gene expression between *Trichodesmium* and its microbiome over day-night cycles in the North Pacific Subtropical Gyre. ISME J 12:997–1007. https://doi.org/10.1038/s41396-017-0041-5
22. Luo W, Luo YW. 2023. Diurnally dynamic iron allocation promotes N_2 fixation in marine dominant diazotroph *Trichodesmium*. Comput Struct Biotechnol J 21:3503–3512. https://doi.org/10.1016/j.csbj.2023.07.006
23. Allen JF. 2003. Cyclic, pseudocyclic and noncyclic photophosphorylation: new links in the chain. Trends Plant Sci 8:15–19. https://doi.org/10.1016/s1360-1385(02)00006-7
24. Geider RJ, Moore CM, Ross ON. 2009. The role of cost–benefit analysis in models of phytoplankton growth and acclimation. Plant Ecology & Diversity 2:165–178. https://doi.org/10.1080/17550870903300949
25. Milligan AJ, Berman - Frank I, Gerchman Y, Dismukes GC, Falkowski PG. 2007. Light - dependent oxygen consumption in nitrogen - fixing cyanobacteria plays a key role in nitrogenase protection. J Phycol 43:845–852. https://doi.org/10.1111/j.1529-8817.2007.00395.x
26. Bergman B, Siddiqui PJA, Carpenter EJ, Peschek GA. 1993. Cytochrome oxidase: subcellular distribution and relationship to nitrogenase

expression in the nonheterocystous marine cyanobacterium *Trichodesmium thiebautii*. Appl Environ Microbiol 59:3239–3244. https://doi.org/10.1128/aem.59.10.3239-3244.1993
27. Kana TM. 1993. Rapid oxygen cycling in *Trichodesmium thiebautii*. Limnology & Oceanography 38:18–24. https://doi.org/10.4319/lo.1993.38.1.0018
28. Staal M, Meysman FJR, Stal LJ. 2003. Temperature excludes N_2-fixing heterocystous cyanobacteria in the tropical oceans. Nature 425:504–507. https://doi.org/10.1038/nature01999
29. Benson BB, Krause D. 1984. The concentration and isotopic fractionation of oxygen dissolved in freshwater and seawater in equilibrium with the atmosphere. Limnology & Oceanography 29:620–632. https://doi.org/10.4319/lo.1984.29.3.0620
30. Bowes G, Ogren WL, Hageman RH. 1971. Phosphoglycolate production catalyzed by ribulose diphosphate carboxylase. Biochem Biophys Res Commun 45:716–722. https://doi.org/10.1016/0006-291x(71)90475-x
31. Flores E, Herrero A. 1994. Assimilatory nitrogen metabolism and its regulation, p 487–517. In Bryant DA (ed), The molecular biology of cyanobacteria. Kluwer Academic Publishers, Dordrecht.
32. Flores E, Frías JE, Rubio LM, Herrero A. 2005. Photosynthetic nitrate assimilation in cyanobacteria. Photosynth Res 83:117–133. https://doi.org/10.1007/s11120-004-5830-9
33. Luo YW, Shi D, Kranz SA, Hopkinson BM, Hong H, Shen R, Zhang F. 2019. Reduced nitrogenase efficiency dominates response of the globally important nitrogen fixer *Trichodesmium* to ocean acidification. Nat Commun 10:1521. https://doi.org/10.1038/s41467-019-09554-7
34. Shi D, Kranz SA, Kim JM, Morel FMM. 2012. Ocean acidification slows nitrogen fixation and growth in the dominant diazotroph *Trichodesmium* under low-iron conditions. Proc Natl Acad Sci USA 109:E3094–100. https://doi.org/10.1073/pnas.1216012109
35. Hong H, Shen R, Zhang F, Wen Z, Chang S, Lin W, Kranz SA, Luo YW, Kao SJ, Morel FMM, Shi D. 2017. The complex effects of ocean acidification on the prominent N_2-fixing cyanobacterium *Trichodesmium*. Science 356:527–531. https://doi.org/10.1126/science.aal2981
36. Gallon JR. 1981. The oxygen sensitivity of nitrogenase: a problem for biochemists and micro-organisms. Trends Biochem Sci 6:19–23. https://doi.org/10.1016/0968-0004(81)90008-6
37. Baker NR, Harbinson J, Kramer DM. 2007. Determining the limitations and regulation of photosynthetic energy transduction in leaves. Plant Cell Environ 30:1107–1125. https://doi.org/10.1111/j.1365-3040.2007.01680.x
38. Pahlow M, Dietze H, Oschlies A. 2013. Optimality-based model of phytoplankton growth and diazotrophy. Mar Ecol Prog Ser 489:1–16. https://doi.org/10.3354/meps10449
39. Leggett RW, Williams LR. 1981. A reliability index for models. Ecol Modell 13:303–312. https://doi.org/10.1016/0304-3800(81)90034-X
40. Stow CA, Jolliff J, McGillicuddy DJ, Doney SC, Allen JI, Friedrichs MAM, Rose KA, Wallhead P. 2009. Skill assessment for coupled biological/physical models of marine systems. J Mar Syst 76:4–15. https://doi.org/10.1016/j.jmarsys.2008.03.011
41. Reimers AM, Knoop H, Bockmayr A, Steuer R. 2017. Cellular trade-offs and optimal resource allocation during cyanobacterial diurnal growth. Proc Natl Acad Sci USA 114:E6457–E6465. https://doi.org/10.1073/pnas.1617508114
42. Zhang F, Hong H, Kranz SA, Shen R, Lin W, Shi D. 2019. Proteomic responses to ocean acidification of the marine diazotroph *Trichodesmium* under iron-replete and iron-limited conditions. Photosynth Res 142:17–34. https://doi.org/10.1007/s11120-019-00643-8
43. Jiang HB, Fu FX, Rivero-Calle S, Levine NM, Sañudo-Wilhelmy SA, Qu PP, Wang XW, Pinedo-Gonzalez P, Zhu Z, Hutchins DA. 2018. Ocean warming alleviates iron limitation of marine nitrogen fixation. Nature Clim Change 8:709–712. https://doi.org/10.1038/s41558-018-0216-8
44. Kranz SA, Eichner M, Rost B. 2011. Interactions between CCM and N_2 fixation in *Trichodesmium*. Photosynth Res 109:73–84. https://doi.org/10.1007/s11120-010-9611-3
45. Boatman TG, Davey PA, Lawson T, Geider RJ. 2019. CO_2 modulation of the rates of photosynthesis and light-dependent O_2 consumption in *Trichodesmium*. J Exp Bot 70:589–597. https://doi.org/10.1093/jxb/ery368
46. Kana TM. 1992. Oxygen cycling in cyanobacteria, with specific reference to oxygen protection in *Trichodesmium* spp, p 29–41. In Carpenter EJ, Capone DG, Rueter JG (ed), Marine pelagic cyanobacteria: *Trichodesmium* and other diazotrophs. Springer Netherlands, Dordrecht.
47. Inomura K, Bragg J, Riemann L, Follows MJ. 2018. A quantitative model of nitrogen fixation in the presence of ammonium. PLOS ONE 13:e0208282. https://doi.org/10.1371/journal.pone.0208282
48. Inomura K, Deutsch C, Wilson ST, Masuda T, Lawrenz E, Lenka B, Sobotka R, Gauglitz JM, Saito MA, Prášil O, Follows MJ. 2019. Quantifying oxygen management and temperature and light dependencies of nitrogen fixation by *Crocosphaera watsonii*. mSphere 4:e00531-19. https://doi.org/10.1128/mSphere.00531-19
49. Großkopf T, Laroche J. 2012. Direct and indirect costs of dinitrogen fixation in *Crocosphaera watsonii* WH8501 and possible implications for the nitrogen cycle. Front Microbiol 3:236. https://doi.org/10.3389/fmicb.2012.00236
50. Inomura K, Bragg J, Follows MJ. 2017. A quantitative analysis of the direct and indirect costs of nitrogen fixation: a model based on *Azotobacter vinelandii*. ISME J 11:166–175. https://doi.org/10.1038/ismej.2016.97
51. Wannicke N, Koch BP, Voss M. 2009. Release of fixed N_2 and C as dissolved compounds by *Trichodesmium erythreum* and *Nodularia spumigena* under the influence of high light and high nutrient (P). Aquat Microb Ecol 57:175–189. https://doi.org/10.3354/ame01343
52. Cai X, Gao K. 2015. Levels of daily light doses under changed day-night cycles regulate temporal segregation of photosynthesis and N_2 fixation in the cyanobacterium *Trichodesmium erythraeum* IMS101. PLOS ONE 10:e0135401. https://doi.org/10.1371/journal.pone.0135401
53. Shao Z, Xu Y, Wang H, Luo W, Wang L, Huang Y, Agawin NSR, Ahmed A, Benavides M, Bentzon-Tilia M, et al. 2023. Global oceanic diazotroph database version 2 and elevated estimate of global oceanic N_2 fixation . Earth Syst Sci Data 15:3673–3709. https://doi.org/10.5194/essd-15-3673-2023
54. Olsen A, Lange N, Key RM, Tanhua T, Bittig HC, Kozyr A, Álvarez M, Azetsu-Scott K, Becker S, Brown PJ, et al. 2020. An updated version of the global interior ocean biogeochemical data product, GLODAPv2.2020. Earth Syst Sci Data 12:3653–3678. https://doi.org/10.5194/essd-12-3653-2020
55. Eichner MJ, Klawonn I, Wilson ST, Littmann S, Whitehouse MJ, Church MJ, Kuypers MM, Karl DM, Ploug H. 2017. Chemical microenvironments and single-cell carbon and nitrogen uptake in field-collected colonies of *Trichodesmium* under different pCO_2 ISME J 11:1305–1317. https://doi.org/10.1038/ismej.2017.15
56. Muñoz-Marín MDC, Shilova IN, Shi T, Farnelid H, Cabello AM, Zehr JP. 2019. The transcriptional cycle is suited to daytime N2 fixation in the unicellular cyanobacterium "*Candidatus* Atelocyanobacterium thalassa(UCYN-A). mBio 10:e02495–18. https://doi.org/10.1128/mBio.02495-18
57. Sáenz JP, Waterbury JB, Eglinton TI, Summons RE. 2012. Hopanoids in marine cyanobacteria: probing their phylogenetic distribution and biological role. Geobiology 10:311–319. https://doi.org/10.1111/j.1472-4669.2012.00318.x
58. Cornejo-Castillo FM, Cabello AM, Salazar G, Sánchez-Baracaldo P, Lima-Mendez G, Hingamp P, Alberti A, Sunagawa S, Bork P, de Vargas C, Raes J, Bowler C, Wincker P, Zehr JP, Gasol JM, Massana R, Acinas SG. 2016. Cyanobacterial symbionts diverged in the late Cretaceous towards lineage-specific nitrogen fixation factories in single-celled phytoplankton. Nat Commun 7:11071. https://doi.org/10.1038/ncomms11071
59. Talbot HM, Summons RE, Jahnke LL, Cockell CS, Rohmer M, Farrimond P. 2008. Cyanobacterial bacteriohopanepolyol signatures from cultures and natural environmental settings. Org Geochem 39:232–263. https://doi.org/10.1016/j.orggeochem.2007.08.006
60. Coale TH, Loconte V, Turk-Kubo KA, Vanslembrouck B, Mak WKE, Cheung S, Ekman A, Chen JH, Hagino K, Takano Y, Nishimura T, Adachi M, Le Gros M, Larabell C, Zehr JP. 2024. Nitrogen-fixing organelle in a marine alga. Science 384:217–222. https://doi.org/10.1126/science.adk1075
61. Cornejo-Castillo FM, Inomura K, Zehr JP, Follows MJ. 2024. Metabolic trade-offs constrain the cell size ratio in a nitrogen-fixing symbiosis. Cell 187:1762–1768. https://doi.org/10.1016/j.cell.2024.02.016
62. Wilson ST, Aylward FO, Ribalet F, Barone B, Casey JR, Connell PE, Eppley JM, Ferrón S, Fitzsimmons JN, Hayes CT, Romano AE, Turk-Kubo KA, Vislova A, Armbrust EV, Caron DA, Church MJ, Zehr JP, Karl DM, DeLong EF. 2017. Coordinated regulation of growth, activity and transcription in natural populations of the unicellular nitrogen-fixing cyanobacterium *Crocosphaera*. Nat Microbiol 2. https://doi.org/10.1038/nmicrobiol.2017.118
63. Cheah YE, Zimont AJ, Lunka SK, Albers SC, Park SJ, Reardon KF, Peebles CAM. 2015. Diel light:dark cycles significantly reduce FFA accumulation

in FFA producing mutants of *Synechocystis* sp. PCC 6803 compared to continuous light. Algal Res 12:487–496. https://doi.org/10.1016/j.algal.2015.10.014
64. Munnik T, Mongrand S, Zársky V, Blatt M. 2021. Dynamic membranes-the indispensable platform for plant growth, signaling, and development. Plant Physiol 185:547–549. https://doi.org/10.1093/plphys/kiaa107
65. Zehr JP. 2011. Nitrogen fixation by marine cyanobacteria. Trends Microbiol 19:162–173. https://doi.org/10.1016/j.tim.2010.12.004
66. Berman-Frank I, Lundgren P, Falkowski P. 2003. Nitrogen fixation and photosynthetic oxygen evolution in cyanobacteria. Res Microbiol 154:157–164. https://doi.org/10.1016/S0923-2508(03)00029-9
67. Zehr JP, Capone DG. 2020. Changing perspectives in marine nitrogen fixation. Science 368:eaay9514. https://doi.org/10.1126/science.aay9514
68. Gao M, Andrews J, Armin G, Chakraborty S, Zehr JP, Inomura K. 2024. Rapid mode switching facilitates the growth of *Trichodesmium*: a model analysis. iScience 27:109906. https://doi.org/10.1016/j.isci.2024.109906
69. Tripp HJ, Bench SR, Turk KA, Foster RA, Desany BA, Niazi F, Affourtit JP, Zehr JP. 2010. Metabolic streamlining in an open-ocean nitrogen-fixing cyanobacterium. Nature 464:90–94. https://doi.org/10.1038/nature08786
70. Welsh EA, Liberton M, Stöckel J, Loh T, Elvitigala T, Wang C, Wollam A, Fulton RS, Clifton SW, Jacobs JM, Aurora R, Ghosh BK, Sherman LA, Smith RD, Wilson RK, Pakrasi HB. 2008. The genome of Cyanothece 51142, a unicellular diazotrophic cyanobacterium important in the marine nitrogen cycle. Proc Natl Acad Sci USA 105:15094–15099. https://doi.org/10.1073/pnas.0805418105
71. Saito MA, Bertrand EM, Dutkiewicz S, Bulygin VV, Moran DM, Monteiro FM, Follows MJ, Valois FW, Waterbury JB. 2011. Iron conservation by reduction of metalloenzyme inventories in the marine diazotroph *Crocosphaera watsonii* . Proc Natl Acad Sci USA 108:2184–2189. https://doi.org/10.1073/pnas.1006943108
72. Masuda T, Inomura K, Mareš J, Prášil O. 2022. *Crocosphaera watsonii*. Trends Microbiol 30:805–806. https://doi.org/10.1016/j.tim.2022.02.006
73. Masuda T, Inomura K, Takahata N, Shiozaki T, Sano Y, Deutsch C, Prášil O, Furuya K. 2020. Heterogeneous nitrogen fixation rates confer energetic advantage and expanded ecological niche of unicellular diazotroph populations. Commun Biol 3:172. https://doi.org/10.1038/s42003-020-0894-4
74. Sáenz JP. 2010. Hopanoid enrichment in a detergent resistant membrane fraction of *Crocosphaera watsonii*: Implications for bacterial lipid raft formation. Org Geochem 41:853–856. https://doi.org/10.1016/j.orggeochem.2010.05.005
75. Schouten S, Villareal TA, Hopmans EC, Mets A, Swanson KM, Sinninghe Damsté JS. 2013. Endosymbiotic heterocystous cyanobacteria synthesize different heterocyst glycolipids than free-living heterocystous cyanobacteria. Phytochemistry 85:115–121. https://doi.org/10.1016/j.phytochem.2012.09.002
76. Garg R, Maldener I. 2021. The dual role of the glycolipid envelope in different cell types of the multicellular cyanobacterium *Anabaena variabilis* ATCC 29413. Front Microbiol 12:645028. https://doi.org/10.3389/fmicb.2021.645028
77. Berman-Frank I, Quigg A, Finkel ZV, Irwin AJ, Haramaty L. 2007. Nitrogen ‐ fixation strategies and Fe requirements in cyanobacteria. Limnology & Oceanography 52:2260–2269. https://doi.org/10.4319/lo.2007.52.5.2260